Electronic Supplementary Information

Sunlight-Assisted, Biocatalytic Formate Synthesis from CO_2 and Water Using Silicon-Based Photoelectrochemical Cell

Eun Jin Son[a], *Jong Wan Ko*[a], *Su Keun Kuk*[a], *Hyunjun Choe*[b], *Sumi Lee*[b], *Jae Hong Kim*[a], *Dong Heon Nam*[a], *Gyeong Min Ryu*[a], *Yong Hwan Kim*[b,]*, *Chan Beum Park*[a,]*

Experimental Details

Materials

Chemicals including cobalt nitrate hexahydrate ($Co(NO_3)_2 \cdot 6H_2O$), hydrofluoric acid (HF), silver nitrate ($AgNO_3$), hydrogen peroxide (H_2O_2), nitric acid (HNO_3), sulfuric acid (H_2SO_4), ß-nicotinamide adenine dinucleotide hydrate (NAD^+), and formate dehydrogenase from *Candida boidinii* (CbFDH) were purchased from Sigma-Aldrich (USA). The Rh-based organometallic electron mediator (**M;** $[Cp^*Rh(bpy)(H_2O)]^{2+}$, $Cp^*=C_5Me_5$, bpy=2,2’-bipyridine) was synthesized according to the literature.[1]

Photoelectrode fabrication

The 3-jn-Si/ITO/CoPi photoanode was fabricated by electrodeposition of CoPi onto 3-jn-Si/ITO. The synthesized 3-jn-Si/ITO (0.8 x 2 cm^2) was immersed in 40 ml of 100 mM KPi buffer (pH 7) solution containing 0.5 mM $Co(NO_3)_2 \cdot 6H_2O$ in a three-electrode voltammetry configuration (3-jn-Si/ITO working electrode, Ag/AgCl reference electrode, and Pt wire counter electrode). Afterward, external bias of 0.9 V was applied for different time periods to deposit CoPi onto the 3-jn-Si/ITO surface. Note that CoPi was deposited on the ITO side. As the deposition time was increased from 5 to 10, 30, and 60 min, the amount of charge passed during the electrodeposition of CoPi was increased from 3.1 to 5.6, 14.0, and 31.4 mC/cm^2, respectively (data not shown). With the increasing deposition time from 5 to 10, and 30 min, the onset potential for water oxidation was cathodically shifted. However, the increase in the onset potential was observed with the deposition time of 60 min, which was attributed to the limitation of hole transport within thick CoPi film, reducing the catalytic effect on water oxidation (**Figure S4**). Hence, we used 30 min deposition samples throughout the experiments. The H-SiNW photocathode was synthesized by a metal-assisted solution etching method. Briefly, a p-type silicon wafer (1 x 7 cm^2) was washed with acetone, ethanol, 2-propanol, and piranha solutions for 5 min each. The silicon wafer was washed with deionized water several times and immersed in 5% HF solution for 3 min. Without rinsing, the wafer was put into a solution of 5 mM $AgNO_3$ and 4.8 M HF for 1 min, followed by rinsing sufficiently with deionized water. Then, the wafer was placed in solution of 0.4 M H_2O_2 and 4.8 M HF for 30 min under dark conditions. After cleaning with deionized water several times, the silicon wafer was immersed in HNO_3 and water (5:5) solution for 1 hr to remove the remaining silver nanoparticles. Afterwards, the wafer was cut into 1 x 1 cm^2 pieces and was made into electrodes by connecting copper wires using carbon paste covered with insulating epoxy resin. Before every use of the H-SiNW photocathode, it was treated with 5% HF solution for 5 min in order to terminate the surface with hydrogen.

Photoelectrochemical NADH regeneration

To perform NADH photoregeneration, H-SiNW photocathode (1 x 1 cm^2) was immersed in a 100 mM phosphate buffer solution (pH 7.0, 10 ml) containing the 1 mM NAD^+, and 250 µM **M** under light illumination (450 W Xe lamp with a 420 nm cut-off filter). According to the cyclic voltammogram analysis, shown in **Figure S10**, the maximum increase of cathodic current was observed with 250 µM of **M**, and there was no further increase with 500 µM of **M**. Thus, we used 250 uM of **M** throughout the experiment considering the maximum electron injection from H-SiNWs to **M**. The water oxidation reaction for supplying electrons to H-SiNWs was carried out in a 50 mM phosphate buffer solution (pH 7.0, 15 ml) irradiated using another 450 W Xe lamp with a 420 nm cut-off filter. Note that the solution for NADH photoregeneration was directly connected to the solution for water oxidation by a salt bridge in a two-electrode voltammetry configuration (3-jn-Si/ITO/CoPi working electrode and H-SiNW counter electrode). The photoelectrochemical NADH regeneration test was carried out for 3 hr until the generated amount of NADH was saturated. During the reaction, the regenerated NAD^+ concentration was determined by observing the peak intensity of absorption spectra at 340 nm using a V-650 spectrophotometer (JASCO Inc., Japan). In the case of one-pot NADH photoregeneration, the photoanode and the photocathode were immersed in the same reaction mixture with 1 mM NAD^+ and 250 μM Rh-based electron mediator in a pH 7.0 phosphate buffer (100 mM). Note that visible light was illuminated to the n-side (i.e., opposite side of deposited CoPi) of 3-jn-Si/ITO/CoPi photoanode to avoid light-blocking effect by CoPi layer and to achieve enhanced photocurrent.

Biocatalytic CO_2 reduction to formate using water as an electron donor

Biocatalytic formate production using CO_2 as a carbon source and water as an electron donor was performed in a two-electrode configuration, where two separated compartments for water oxidation and CO_2 reduction were connected by salt bridge. For water oxidation, the 3-jn-Si/ITO/CoPi photoanode was immersed in a 50 mM phosphate buffer (pH 7.0, 15 ml) and for formate production, H-SiNW was immersed in the reaction mixture (pH 6.8, 100 mM phosphate buffer) that contained 1 mM NAD^+, 250 μM Rh-based electron mediator, and 3 mg of TsFDH under continuous CO_2 bubbling. Note that the 100 mM phosphate buffer solution was saturated with CO_2 gas before the addition of the other reaction components. After the CO_2 saturation, pH value of the buffer was slightly decreased from 7.0 to 6.8. The water oxidation and CO_2 reduction reactions were performed at 32 ℃, which is maintained by a water bath. The other experimental setup was the same as the photoelectrochemical NADH regeneration. Formate concentration was determined by calculating the area of formate peak from the sample solution diluted by H_2SO_4 for inactivation of the TsFDH, and the peak was detected using liquid chromatography (LC-20A, prominence, Shimadzu, Japan) equipped with an Aminex® HPX-87H ion exclusion column. In order to investigate the contribution of each photoelectrode, CO_2 fixation was carried out with the same experimental set-up as the full-cell system, except 3-jn-Si/ITO/CoPi working electrode with Pt counter electrode, or Pt working electrode with H-SiNW counter electrode. The Faradaic efficiency for formate was calculated according to the following equation:

$$\text{Faradaic efficiency} = \frac{\text{amount of formate (moles)} \times n \times F}{Q} \times 100\ (\%)$$

where n is the number of electrons needed for formate production, F is Faraday’s constant, and Q is the charge passed during the reaction.

Characterization

The morphology and elemental analysis of 3-jn-Si/ITO/CoPi and H-SiNW were examined by scanning electron microscopy and energy dispersive X-ray (Hitachi High-Technologies Co., Japan). Electrochemical measurement of both the full-cell and half-cells were carried out in pH 7.0 phosphate buffer (50 mM for 3-jn-Si/ITO/CoPi photoanode and 100 mM for H-SiNW photocathode) using potentiostat/galvanostat (WonATech, Model WMPG1000, Korea). Note that half-cells are consisted of a Pt counter electrode, a Ag/AgCl counter electrode, and the 3-jn-Si/ITO/CoPi or H-SiNW working electrode. Cyclic voltammetry and linear-sweep voltammetry were scanned at a rate of 50 mV/s. The photocurrent measurement of the full-cell under chopped illumination was conducted at a time interval of 30 sec.

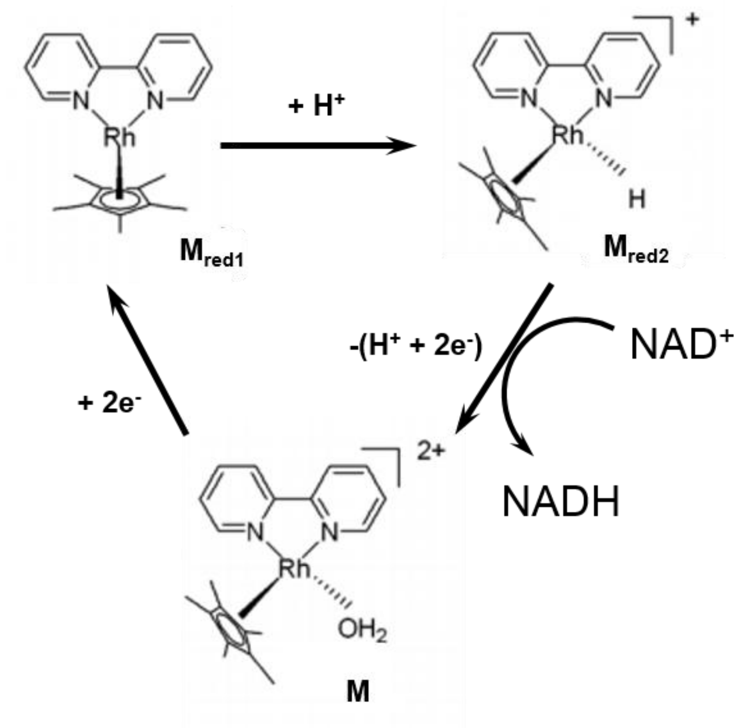

Figure S1. Schematic illustration of molecular structure of three different electrochemical states of Rh-based organometallic electron mediator {**M;** $[Cp^{*}Rh(bpy)(H_2O)]^{2+}$, $Cp^{*}=C_5Me_5$, bpy=2,2'-bipyridine}.[1]

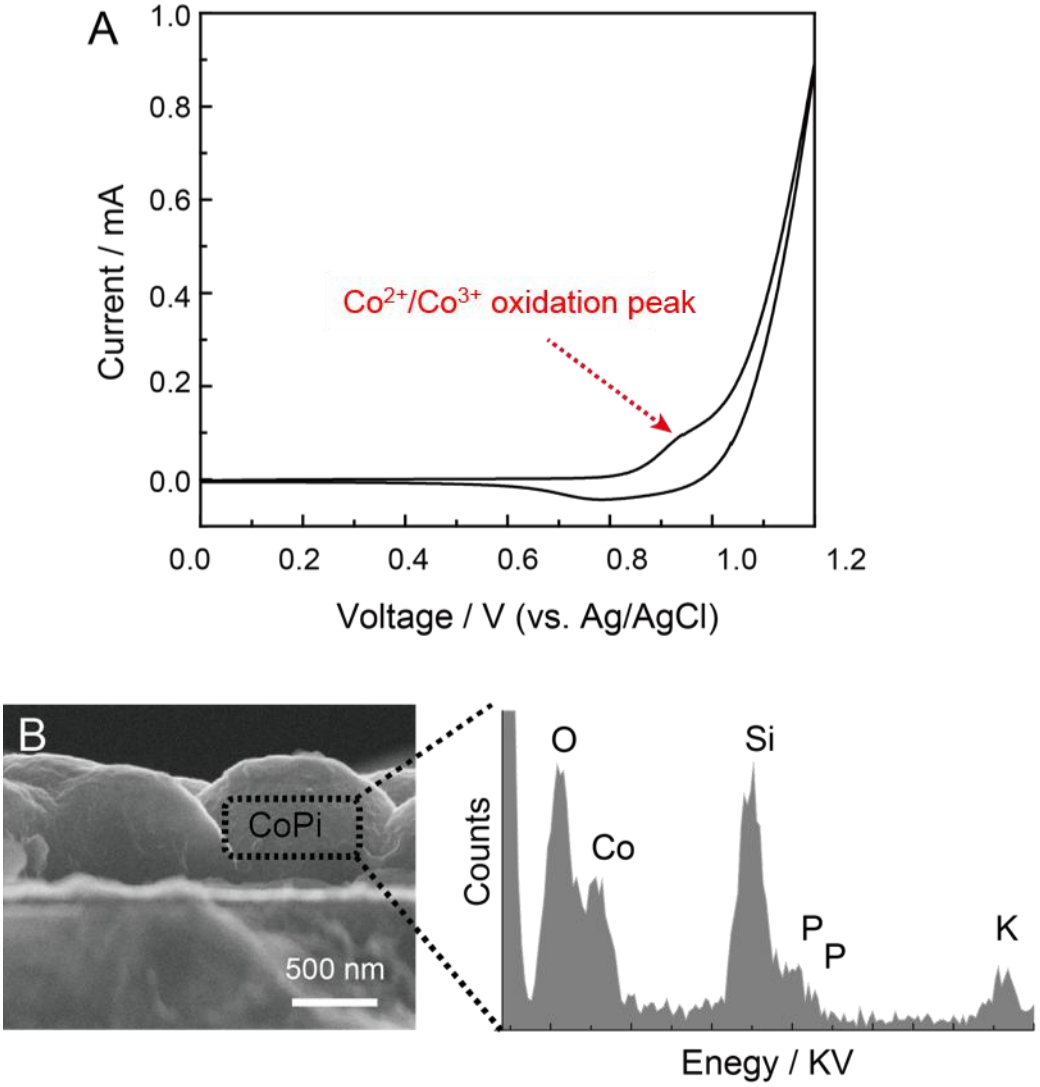

Figure S2. (A) Cyclic voltammogram of 0.5 mM cobalt ion solution in pH 7 KPi buffer (100 mM). According to the Co^{2+}/Co^{3+} oxidation peak at 0.9 V (vs. Ag/AgCl), cobalt phosphate (CoPi) electrodeposition was performed at the same voltage. (B) SEM image of the deposited CoPi and the corresponding EDX spectrum. Note that the deposition time was 60 min.

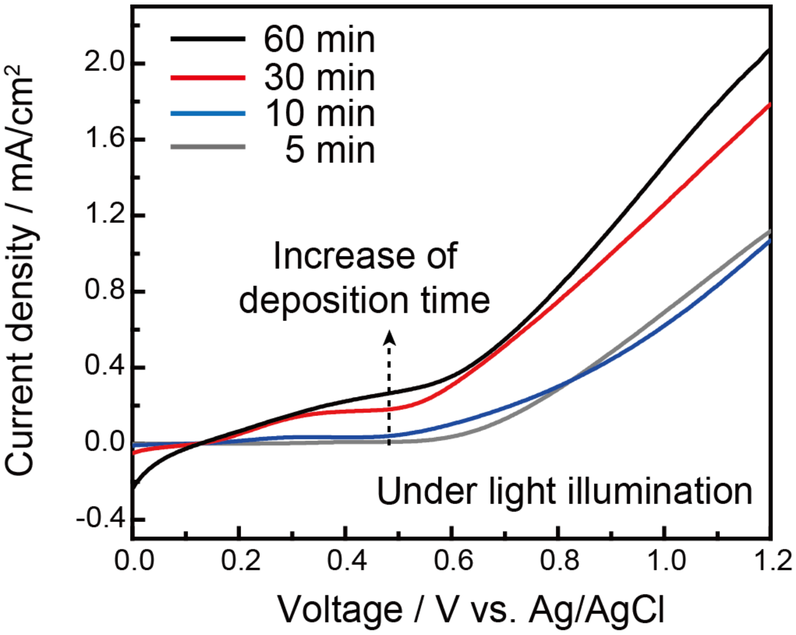

Figure S3. Linear-sweep voltammogram of 3-jn-Si/ITO/CoPi photoanode under light irradiation with different deposition times. Scan rate was 50 mV/s.

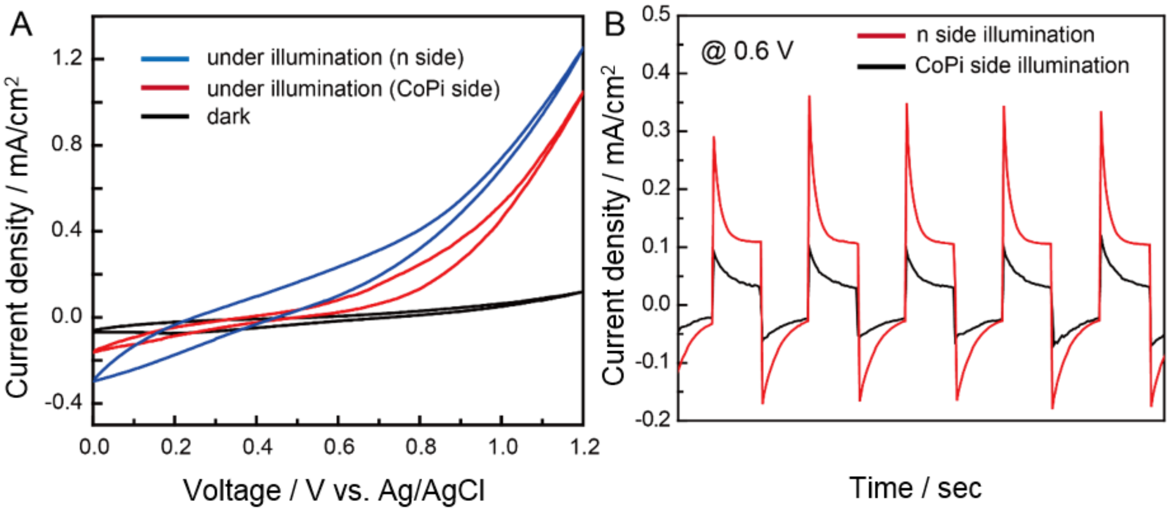

Figure S4. Illumination direction-dependent (A) cyclic voltammetric characteristics of the CoPi-deposited 3-jn-Si/ITO (3-jn-Si/ITO/CoPi) and (B) photocurrent density of the 3-jn-Si/ITO/CoPi photoanode at an applied bias of 0.6 V. The photocurrent measurement of the full-cell under chopped illumination was conducted at a time interval of 30 sec.

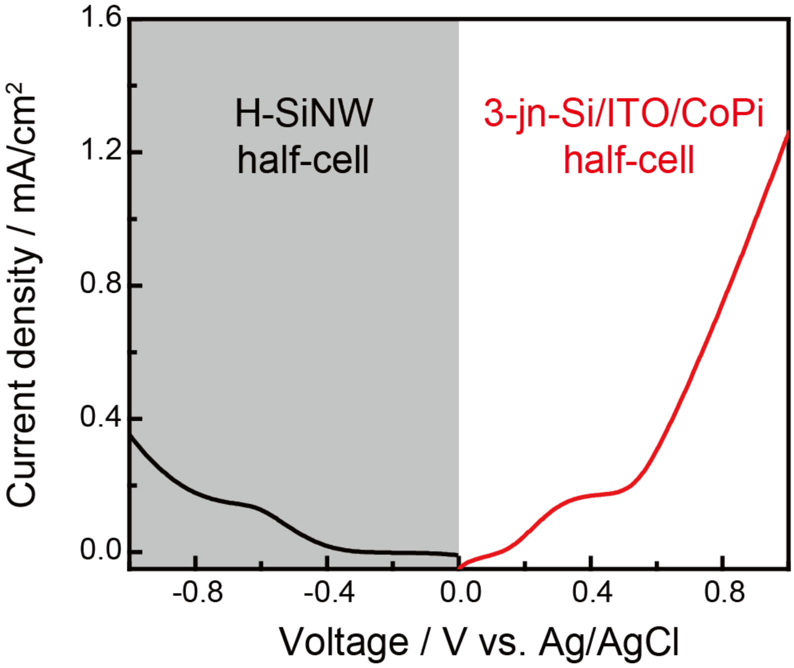

Figure S5. Overlapping of the J-V cureves of each photoelectrode half-cell. The electrochemical measurement was performed in pH 7.0 phosphate buffer in a three-electrode configuration. Scan rate was 50 mV/s.

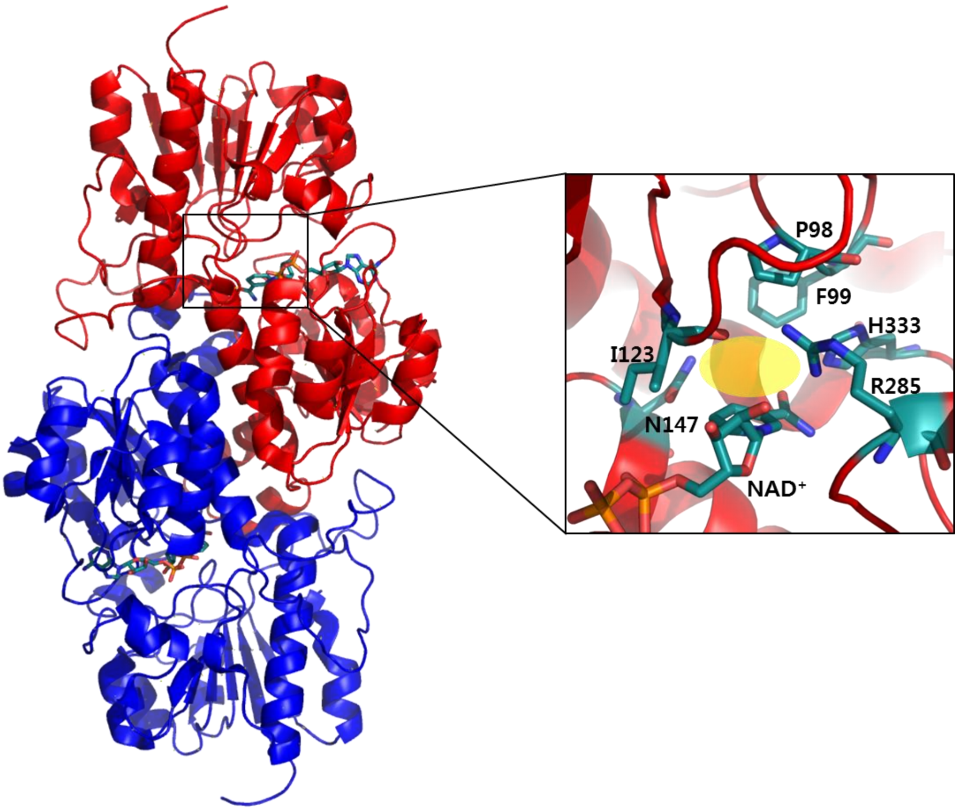

Figure S6. Schematic illustration of dimer structure of TsFDH. Monomers A and B are colored red and blue, respectively. The crystal structure of the TsFDH-NAD$^+$ complex consists of 20 α-helices and 13 β-strands and contains two globular domains. The zoom-in figure demonstrates the binding mode of NAD$^+$ in the active site of TsFDH. It has been suggested that substrate (i.e., CO_2) captured by Lys287 in TsFDH is delivered to active site of NADH-binding TsFDH. Afterward, CO_2 is further stabilized by Arg285 and TsFDH releases NAD$^+$ and formate. The PDB reference number of TsFDH is 3wr5.

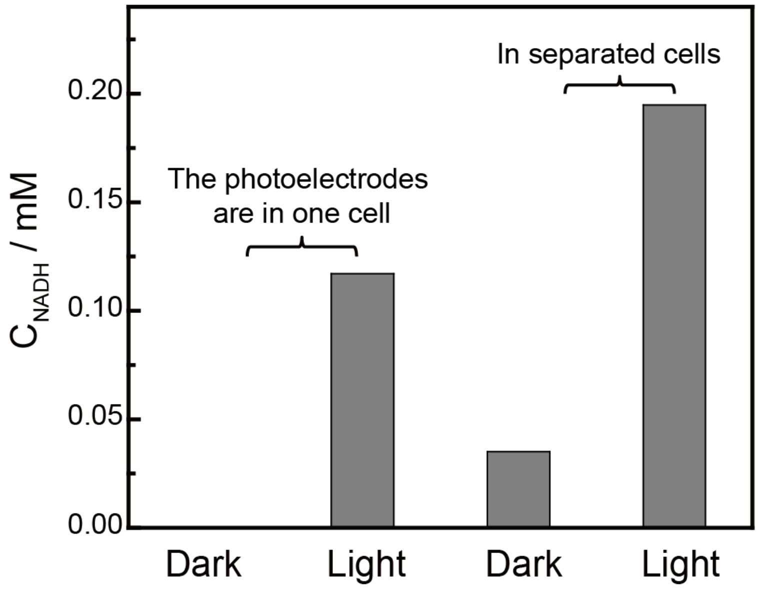

Figure S7. The yields of NADH regeneration by the full PEC cell at separate and combined configurations under dark and light conditions with an applied bias of 1.8 V in a two-electrode configuration. The 3-jn-Si/ITO/CoPi photoanode was immersed in a 50 mM phosphate buffer (pH 7.0, 15 ml) and the H-SiNW was immersed in the reaction mixture (pH 7.0, 100 mM phosphate buffer) that contained 1 mM NAD^+, 250 µM Rh-based electron mediator.

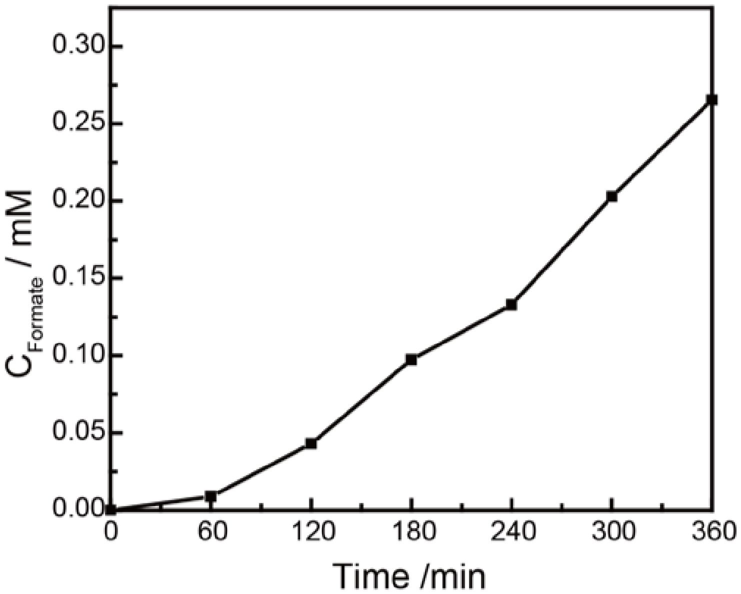

Figure S8. Time profiles for foromate production by the all-silicon-based cell in a 2-electrode configuration, where two separated compartments for water oxidation and CO_2 reduction were connected by salt bridge. For water oxidation, the 3-jn-Si/ITO/CoPi photoanode was immersed in a 50 mM phosphate buffer (pH 7.0, 15 ml) and for formate production, H-SiNW was immersed in the reaction mixture (pH 6.8, 100 mM phosphate buffer) that contained 1 mM NAD^+, 250 µM Rh-based electron mediator, and 3 mg of TsFDH under continuous CO_2 bubbling. The temperature was maintained at 32 °C.

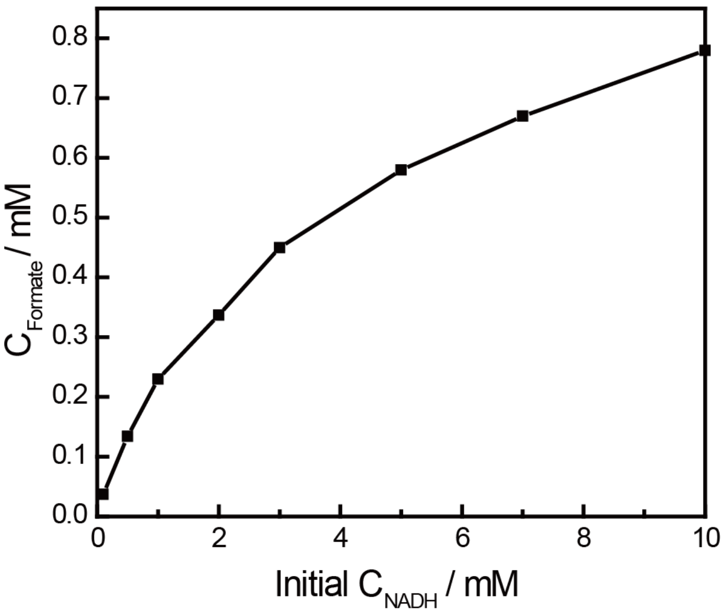

Figure S9. The equilibrium formate concentrations in terms of different initial NADH concentrations. Note that NADH used here is not synthesized from regeneration system. The CO_2 reduction reaction was performed using 2 mg of TsFDH in 100 mM PB buffer (pH 7, 10 ml) at 30 °C with continuous CO_2 purging with the flow rate of 50 ml min^{-1}.

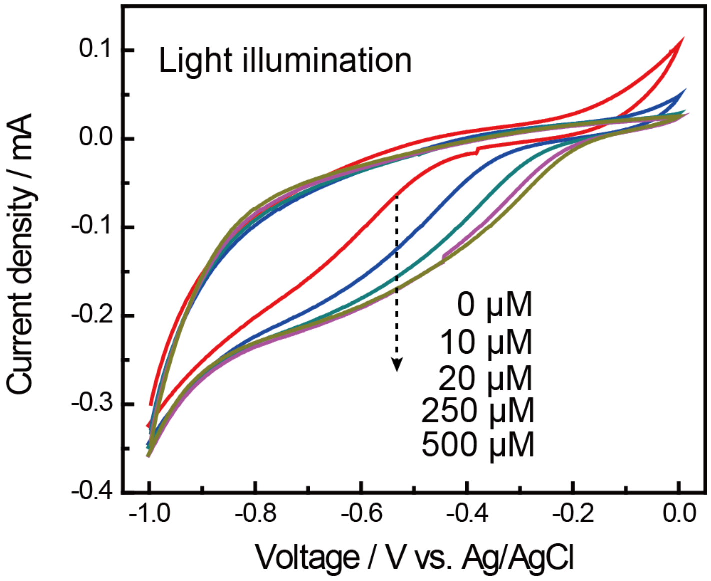

Figure S10. Comparison of cathodic current densities of the H-SiNW photocathode at different concentrations of **M** under light illumination. The maximum increase of cathodic current was observed with 250 μM of **M**, and there was no further increase with 500 μM of **M**. Thus, we used 250 μM of **M** throughout the experiment, considering the maximum electron injection from H-SiNWs to **M**.

Reference for Supporting Information

[1] a) H.-K. Song, S. H. Lee, K. Won, J. H. Park, J. K. Kim, H. Lee, S.-J. Moon, D. K. Kim, C. B. Park, *Angew. Chem. Int. Edit.* **2008**, *47*, 1749; b) E. Steckhan, S. Herrmann, R. Ruppert, E. Dietz, M. Frede, E. Spika, *Organometallics* **1991**, *10,* 1568.